



HAL
open science

Grease composition influence on friction & starvation

Valentin Ripard, David Gonçalves, Fabrice Ville, Jorge H. O. Seabra, Jérôme Cavoret, Pierre Charles

► **To cite this version:**

Valentin Ripard, David Gonçalves, Fabrice Ville, Jorge H. O. Seabra, Jérôme Cavoret, et al.. Grease composition influence on friction & starvation. Proceedings of the Institution of Mechanical Engineers, Part J: Journal of Engineering Tribology, 2021, 236 (7), pp.1336-1349. 10.1177/13506501211059341 . hal-03660200

HAL Id: hal-03660200

<https://hal.science/hal-03660200>

Submitted on 12 May 2023

HAL is a multi-disciplinary open access archive for the deposit and dissemination of scientific research documents, whether they are published or not. The documents may come from teaching and research institutions in France or abroad, or from public or private research centers.

L'archive ouverte pluridisciplinaire **HAL**, est destinée au dépôt et à la diffusion de documents scientifiques de niveau recherche, publiés ou non, émanant des établissements d'enseignement et de recherche français ou étrangers, des laboratoires publics ou privés.



Distributed under a Creative Commons Attribution 4.0 International License

Grease composition influence on friction & starvation

V. Ripard¹, D. Goncalves², F. Ville¹, J.H.O. Seabra³,
J. Cavoret¹ and P. Charles⁴

Abstract

Nowadays, grease lubrication is frequently used in rolling element applications such as bearings or constant velocity joints. The advantage of grease is to supply lubrication to the application without leaking thanks to its consistency. Nevertheless, starvation can occur leading to damage such as scuffing. In the present study, starvation is analyzed using the Starvation Degree parameter through tests with different operating conditions and different types of greases.

Keywords

Tribology, grease, lubrication, film thickness, starvation

Introduction

Greases are mainly used to lubricate components such as rolling element bearings or drivetrain components. The lubrication mechanism is quite complex.¹ It seems that grease lubrication is not a continuous process but it is characterized by events caused by film breakdown and recovery.²

In order to study the lubrication mechanism and possible starvation, film thickness is measured using different techniques such as electrical conductivity³ or interferometry⁴ on a ball on disc tribometer for example. Using these techniques, base oil viscosity appears not to be enough to evaluate film thickness. The thickener must be taken into account especially at low speed.⁵ The thickener structure in particular plays a key factor on film thickness.⁶

Relubrication is a key parameter to extend bearing life at low temperature. In addition, the mechanical design of the component also plays an important role.⁷ If relubrication is poor, starvation could occur. To evaluate starvation risk, a single dimensionless parameter (SD), between the operating parameters and the transition from the fully flooded to starved regime in case of oil lubricating contact was developed.⁸ Its parameters are surface tension effects σ_S , amount of oil present in the vicinity of the track $h_{oil\infty}$, base oil viscosity η_0 , the track width a and the velocity u . It gives the formula below:

$$SD = \frac{\eta_0 ua}{h_{oil\infty}\sigma_S}$$

For greased lubricated contacts, the SD evaluation is quite

complicated due to events as mentioned before.⁹ Nevertheless, film recovery was often observed even if starvation occurs.¹⁰ It seems to be due to contact oscillations that help film thickness recovery up to fully flooded conditions.

In the present paper, different greases in terms of composition and physical or chemical properties were tested using different tribometers. Starvation and the SD parameter are analysed using different operating conditions such as temperatures and/or speeds.

1. Material and methods

1.1. Grease properties

Four greases were used. Their compositions vary (Table 1). Two base oils are used. The first one (A) is a mix between PAO and mineral oil. The second one (B) is a synthetic one. Two different thickeners technologies are used. The first one is a complex soap using Lithium and Calcium. The second one uses polyurea thickener.

¹Univ Lyon, INSA-Lyon, LaMCoS, France

²INEGI, Universidade do Porto, Porto, Portugal

³FEUP, Universidade do Porto, Porto, Portugal

⁴STELLANTIS, Velizy technical center, France

Corresponding author:

V Ripard, Univ Lyon, INSA-Lyon, CNRS UMR5259, LaMCoS, F-69621, France.

Email: valentin.ripard@insa-lyon.fr

Table 1. composition of greases tested.

	G1	G2	G3	G4
Oil	A (Mineral + PAO)	A (Mineral + PAO)	B (Synthetic ester + PAO)	B (Synthetic ester + PAO)
Thickener	Lithium / Calcium Complex	Lithium / Calcium Complex	Polyurea	Polyurea
Additives	MODTC 0,28	MODTC 1 MODTP 0,4	MODTC 1 MODTP 0,4	MODTC 1 MODTP 0,4
Base oil dynamic viscosity μ_0 (cP) 40°C	58.2	58.2	64.2	64.2
Base oil dynamic viscosity μ_0 (cP) 80°C	11.1	11.1	13.5	13.5
S_Oil (%) IP 121 ¹²	3.6	3.6	0.6	6
NLGI number ²²	2	2	1-2	1-2

Four greases were used. Their compositions vary (table 1).

However, even if G3 & G4 have same thickener technology, the manufacturing process changes. To finish, two types of additives¹¹ are used : MoDTC (Molybdenum Dithiocarbamates), MoDTP (Molybdenum Dithiophosphate). Concentrations were normalized to 1 for the maximum additive concentration.

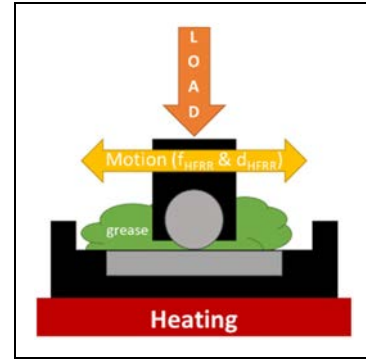
Moreover, the oil separation from lubricating grease is determined on greases using IP121 method.¹² For 42 h at 40°C, greases are inside cups in order to separate the oil from the grease. A mass is used in order to press the grease into cup. The oil is salvaged in a container.

As expected, G1 and G2 give the same oil separation results because only additives were added between G1 & G2. On the contrary, it is possible to observe a huge gap between G3 and G4. Even if the components are the same, different oil separation results are obtained which will influence their properties. It is due to the completely different manufacturing process of the thickener.

1.2. High frequency reciprocating rig

A PCS instrument HFRR is used to study the different available greases. The HFRR allows to measure friction coefficient and separation rate of a lubricant. The test principle is to study an alternative contact with pure sliding of a ball on a disc (Figure 1). It allows also to evaluate the grease ability to supply oil in the contact. It is easy to use thanks to its design. Also balls & discs are inexpensive sample. The applied load can be set from 0.98 N –(0.63 GPa) to 9.81 N (1.37 GPa) which applied a pressure named P_{h-HFRR} .

The upper specimen is a 6 mm diameter ball and the bottom specimen a flat disc. They are made from polished 100Cr6 steel with $R_a < 20$ nm for the disc and $R_a < 50$ nm for the ball. The rig can be configured in terms of frequency f_{HFRR} (from 10 Hz to 200 Hz) and stroke d_{HFRR} (from 20 μ m to 2 mm). The temperature can be set from ambient temperature up to 150°C thanks to a heater block placed under the lower specimen.

**Figure 1.** Schematic of the HFRR.**Table 2.** initial HFRR conditions.

Test number	Duration [h]	Temperature [°C]
1	3	40
2	18	40
3	3	80
4	18	80

Test conditions, chosen in order to maximize speed on HFRR are the following:

$$f_{HFRR} = 15\text{Hz} ; d_{HFRR} = 1\text{mm} ;$$

$$P_{h-HFRR} = 1.32\text{ GPa}$$

To conduct this study different test durations and operating temperatures are set (Table 2). For this study, it is possible to write SD as a function of SD_{HFRR} which is assumed constant for this study ($\frac{a}{h_{oil\infty\sigma_S}}$), η_0 & u which variate between tests:

$$SD = \frac{\eta_0 ua}{h_{oil\infty\sigma_S}} = \eta_0 u SD_{HFRR}$$

This condition gives a mean sliding velocity of 30 mm/s. A test example is available in Figure 2.

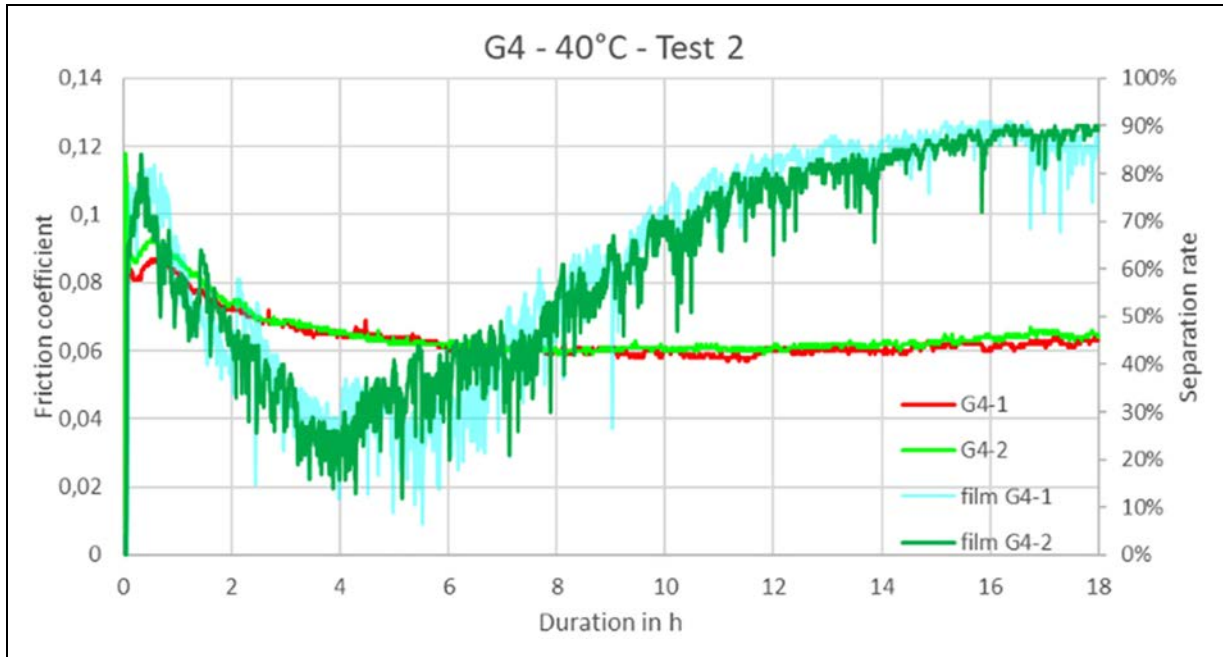


Figure 2. HFRR test example with condition 1.

For test condition 1 with G4 it is possible to observe repeatability between 2 tests (curves G4-1 & G4-2) and also the film thickness corresponding to first friction test. Considering a time t , it is possible to calculate the gap between the friction coefficient G4-1 and G4-2 and divide it by G4-1 value. Taking the mean value, the deviation between these curves is 2%. So, the HFRR test device is a very reliable rig in order to study the friction coefficient with grease.

In addition, to analyse the behaviour of grease during the test, the electrical contact potential is measured to evaluate surface separation.

A second set of tests are considered in Table 3 in order to evaluate starvation. In order to increase the SD parameter, it is possible to increase mean velocity on test rig.

Table 3. New HFRR conditions to discriminate grease starvation.

Test number	f_{HFRR} [Hz]	d_{HFRR} [mm]	P_{h-HFRR} [GPa]	Duration [h]	Temperature [°C]
5	100	2	1.32	3	40
6	80	2	1.32	3	40
7	100	2	1.32	3	80

Table 4. SD ratio variation as function of SD_{G1-3} .

	Test conditions number				
	1 & 2	3 & 4	5	6	7
G1	5.2	1	69.9	55.9	13.3
G2	5.2	1	69.9	55.9	13.3
G3	5.8	1.2	77.1	61.7	16.2
G4	5.8	1.2	77.1	61.7	16.2

Considering, the minimum SD value as SD_{G1-3} , it is possible to calculate variation of SD for each condition. It is expose in Table 4 as a ratio between $\frac{SD}{SD_{G1-3}}$. It is important to note that a higher SD value is more prone to starvation.

The wear scars induced are measured using a Sensofar PLu neox optical profiler with Nikon objectives. Its vertical resolution is less than 0.1 nm. It uses an interferometry technique in order to determine topography.

1.3. Ball-on-disc film thickness

In order to explain the different behaviour of the grease in terms of wear and to complete the rheology study an investigation is carried out using EHD2 from PCS Instruments. It consists of a ball or roller on a disc contact with rolling and/or sliding conditions. This equipment allows to validate first results from HFRR and measure film thickness instead of having film separation. It is also possible to visualize contact and lubricant repartition inside the contact with a camera. The ball and disc are mounted on an independent rotational shaft with speed control S_{EHD} . So, a slide to roll ratio SRR_{EHD} can be introduced inside the contact. It can measure traction coefficient but also the film thickness down to 1 nm. The main goal of that study is to measure the grease film thickness using interferometry.⁴

Samples used are:

- A roller made from 100Cr6 with a minor diameter of 19.05 mm and a crowned diameter of 133.35 mm. Its roughness is down to 20 nm.
- A disc made from glass ($E = 75$ GPa $\nu = 0.2$) with a roughness of approximately 5 nm.

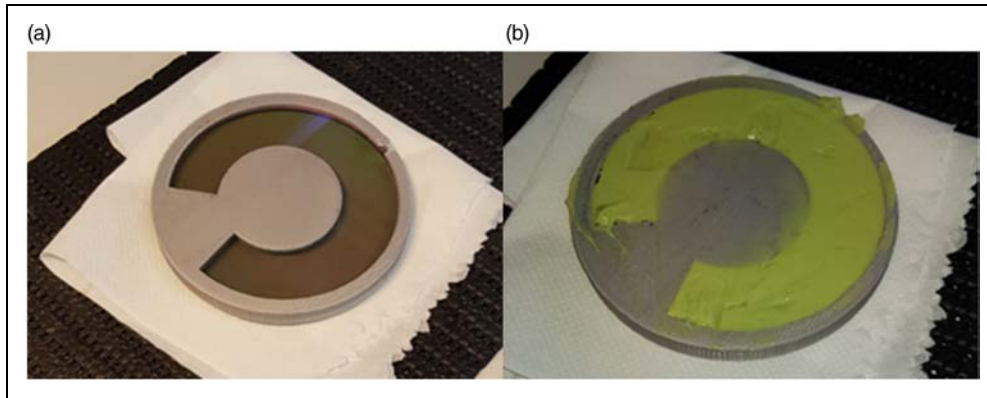


Figure 3. (a) EHD stencil, (b) stencil filled.

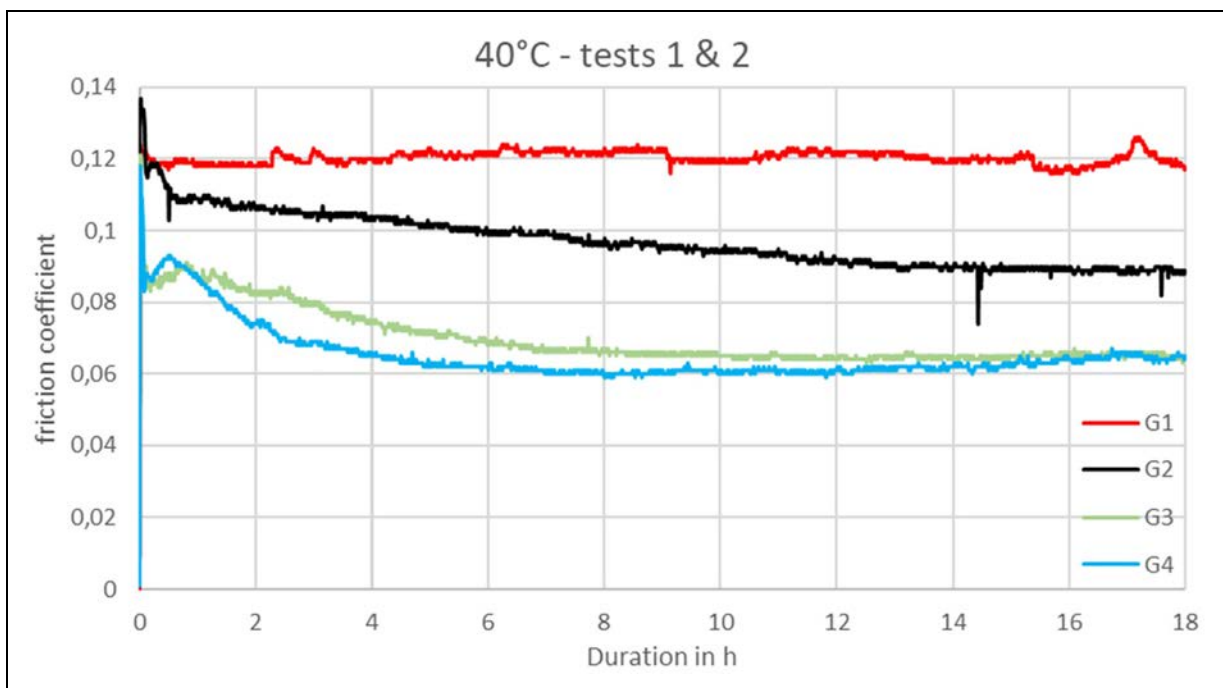


Figure 4. Grease friction coefficient results at 40°C.

Tests are conducted without grease scoop⁹ to go as close as possible to the real contact. To insure repeatability, a 3D printed stencil is used (Figure 3(a)). When the stencil is filled, it allows 7.2 millilitre of grease to be placed on the disc (Figure 3(b)) ensuring that the same volume of grease is used for all the tests.

The tests conditions are available in Table 5. They are set in order to allow maximum load available (so

maximum Contact Hertz Pressure P_{h-EHD}) and a mean velocity equal to conditions 5 & 7.

Compared to HFRR, the speed is almost equivalent to tests 5 & 7. However, EHD2 uses rolling and sliding contact as opposed to HFRR that only uses pure sliding contact. Another difference, is that, even if the load is almost equivalent, one sample is made of glass so the Young's modulus varies a lot. For that reason, hertz pressure drops.

2. Experimental results

2.1. HFRR

2.1.1. Friction at 40°C. The first step is to use HFRR in order to qualify the grease in terms of the friction coefficient and surface separation.

At 40°C, the first observation is the role of additive concentrations. Indeed, the modification of the MODTC

Table 5. EHD test conditions.

Test number	S_{EHD} [mm/s]	SRR_{EHD} [%]	P_{h-EHD} [GPa]	Duration [s]	Temperature [°C]
8	400	10	0.38	2100	40
9	400	10	0.38	2100	80

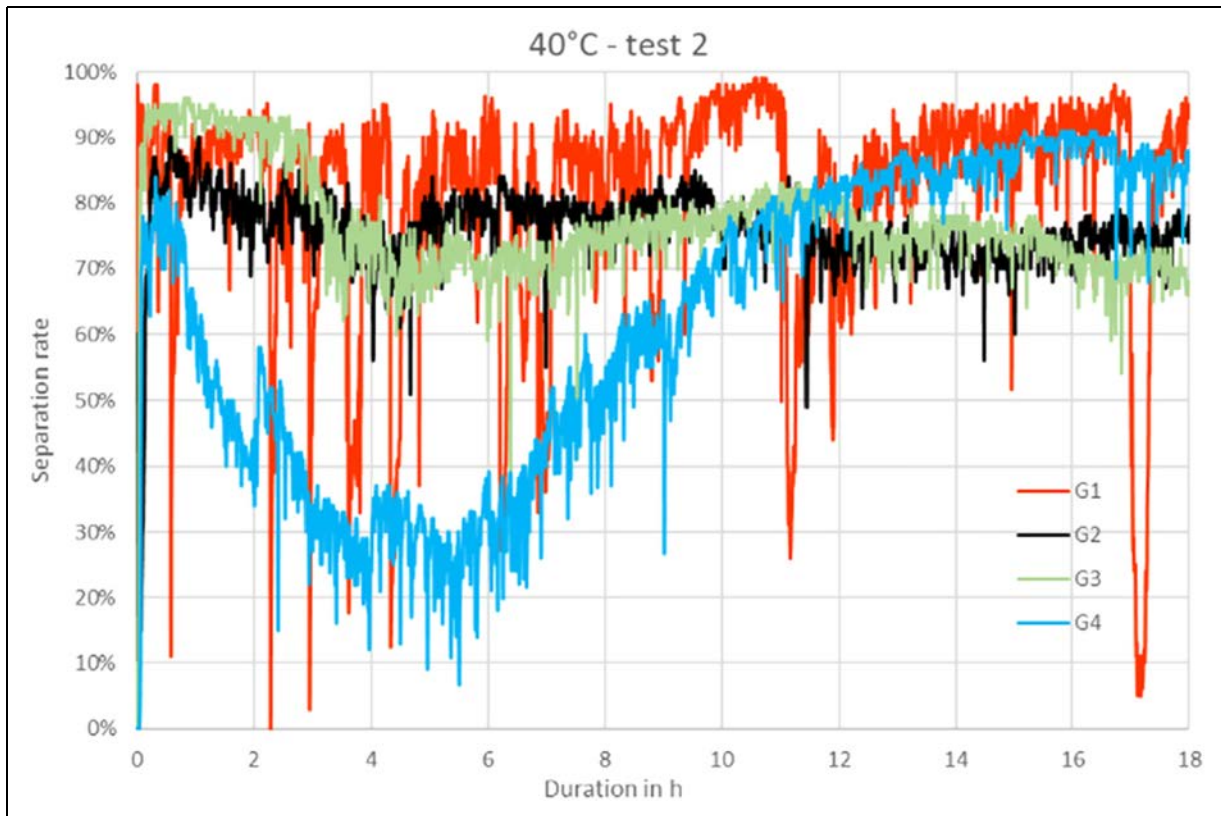


Figure 5. Greases film thickness at 40°C.

concentration and also the addition of MODTP (G1 to G2) allow the friction coefficient to be decreased by 25%, once COF is stabilized (around 16 h). Moreover, the replacement of the thickener and base oil (G2 to G3 & G4) allows the friction coefficient (COF) again to be decreased by 30% in order to give a low friction grease. These 2 major modifications give two types of grease: a low friction grease with a COF of 0.06 and a regular grease with a COF of 0.12 after stabilization.

Figure 5 gives an indication of the separation during tests measuring the electrical resistance between the 2 surfaces.

Separations for greases G2, G3 & G4 vary during tests at the opposite of G1 which is stable from the beginning. The most important is to do not have separation equal to 0 which could mean a dry contact. In this case, separation rate is always above 20%. After the stabilization of the COF, a distinction can be established between the grease with a full additive package (G2, G3, G4) and grease G1 without the same MODTC concentration and MODTP.

In addition, wear scars have been measured and the polyurea grease seems to better protect surfaces.

2.1.2. Friction at 80°C. In Figure 6, the coefficient of friction evolution is represented. For each grease, 2 different durations were set: 3 h and 18 h. The tests were

carried out twice and the curves could be superposed. In order to clarify, only 18 h tests were plotted on Figure 6.

The first observation is that the coefficient of friction of greases G1 & G2 converge around 0.08 to 0.09. However, the G1 friction coefficient seems unstable. An explanation can be that the tribofilm is heterogeneous. Using XPS measurements,¹³ it has been proved that Mo intensity can vary all along the scar width depending on the grease composition Figure 7.

At 80°C, the additive concentration does not have a significant influence on the coefficient of friction, when comparing grease G1 and G2. The low friction greases G3 and G4 have a coefficient of friction below 0.08 which is interesting for a drivetrain application. As an example, a low friction grease will lead to reduce generated axial force on a constant velocity joint.¹⁴ In addition, a friction coefficient increase (G4) is noticed at around 3 h. This increase can be linked to the thickener on G4, the bleed oil from G3 & G4 being the same.

Figure 8 presents the separations of each grease at 80°C which seem to be quite significant.

At 80°C the performance gap between greases becomes less. The concentration of additives seems to be less relevant than at 40°C. However, it is important to notice the couple oil + thickener plays a key role on performance at this temperature.

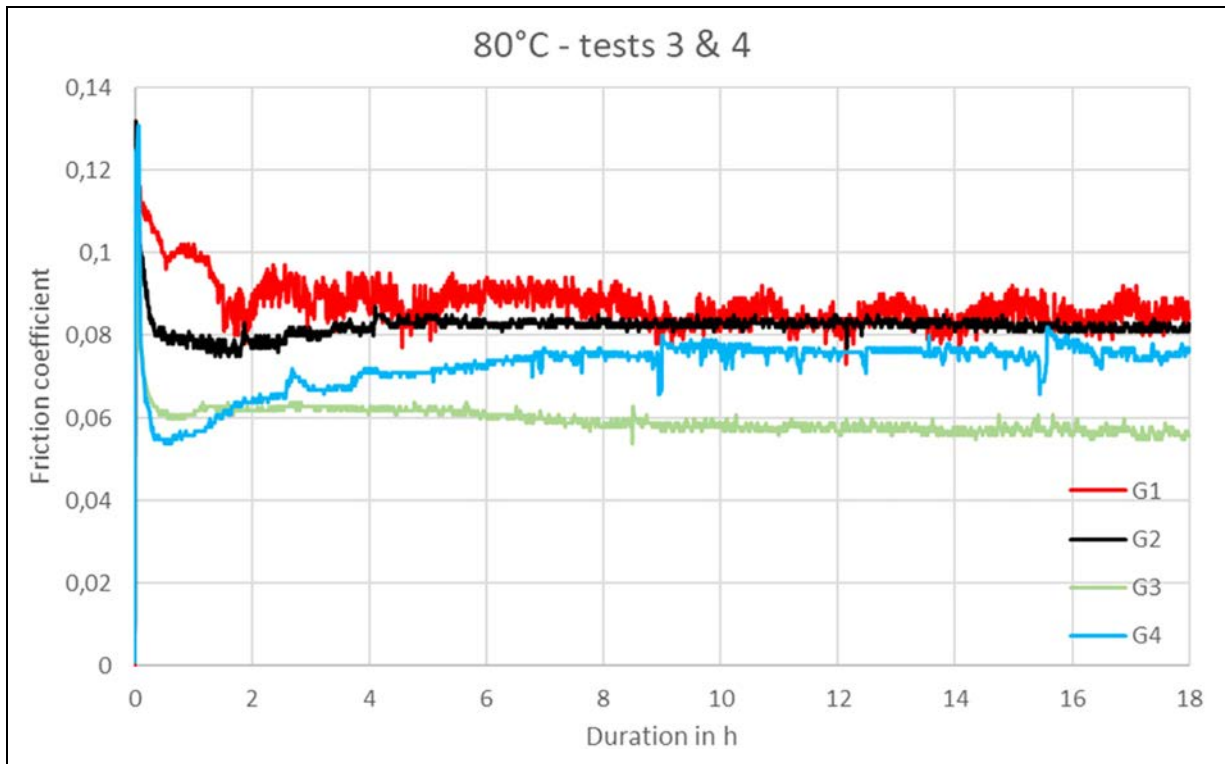


Figure 6. Grease friction coefficient results at 80°C.

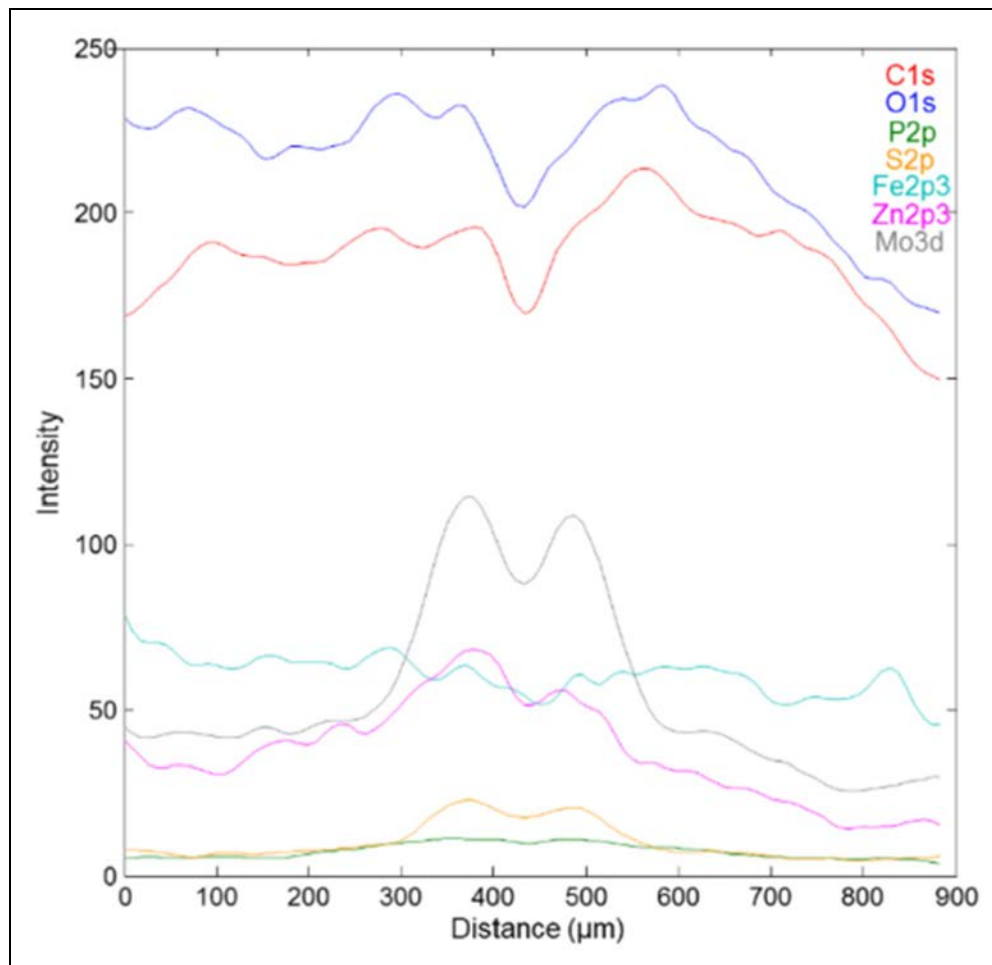


Figure 7. XPS line scan from wear scars with same types of grease.¹³

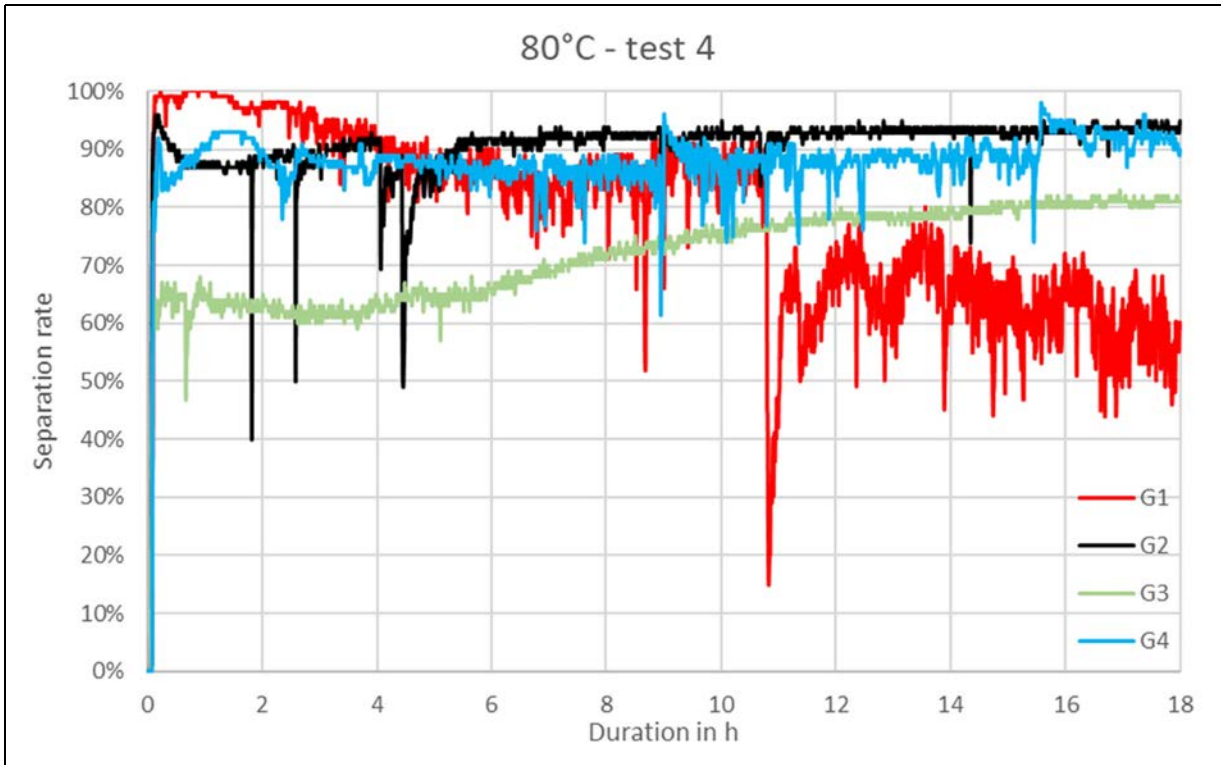


Figure 8. Grease film thickness at 80°C

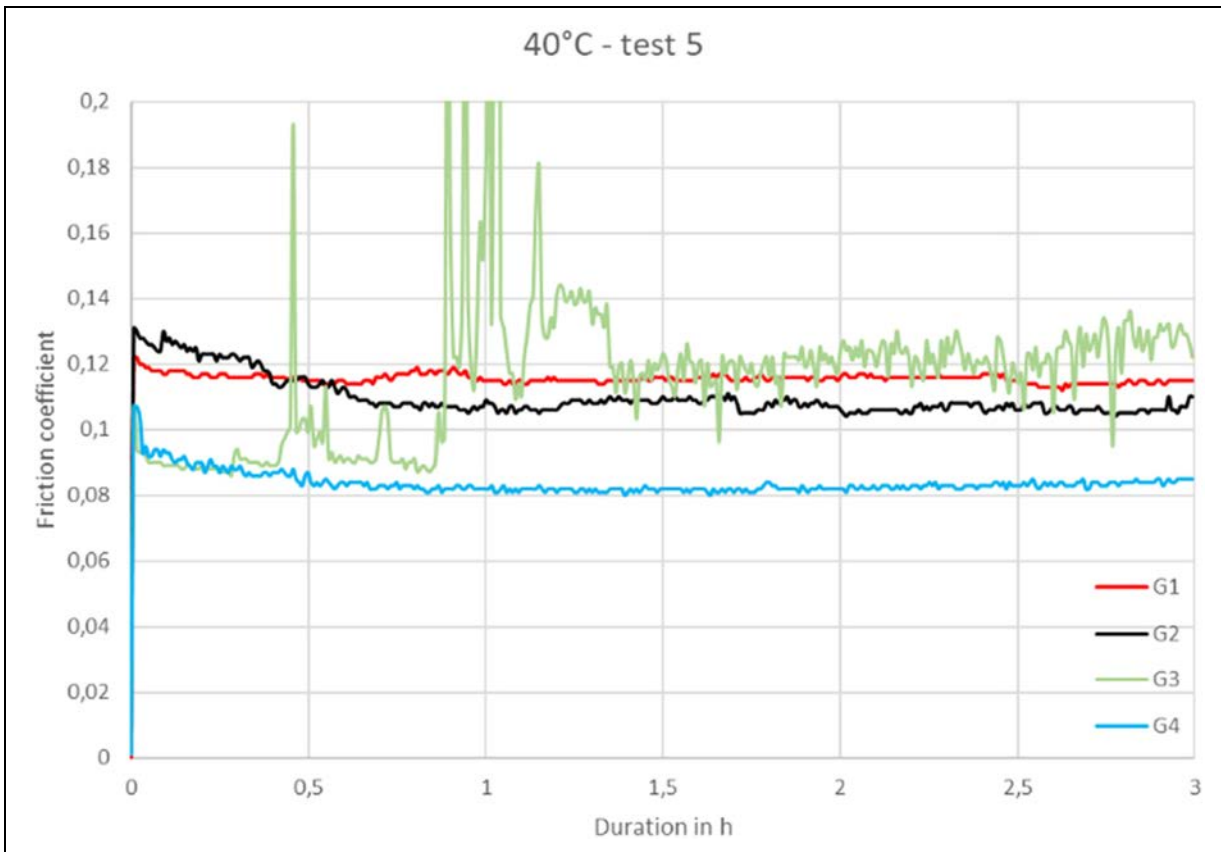


Figure 9. Friction coefficient for test number 5.

2.1.3. *Test operating conditions evolution to provoke starvation.* A first approach is proposed to explain the influence of grease composition on friction. It shows the important role of additives on friction coefficient but also the contribution of the couple thickener + oil. This role is amplified at 40°C as it is possible to observe.

Also, the couple oil + thickener is involved in friction coefficient establishment duration.

In order to induce starvation, test conditions available in Table 3 were used on HFRR. These conditions, increasing frequency from 15 to 100 Hz and distance from 1 to 2 mm, induce a mean sliding speed thirteen times higher which can

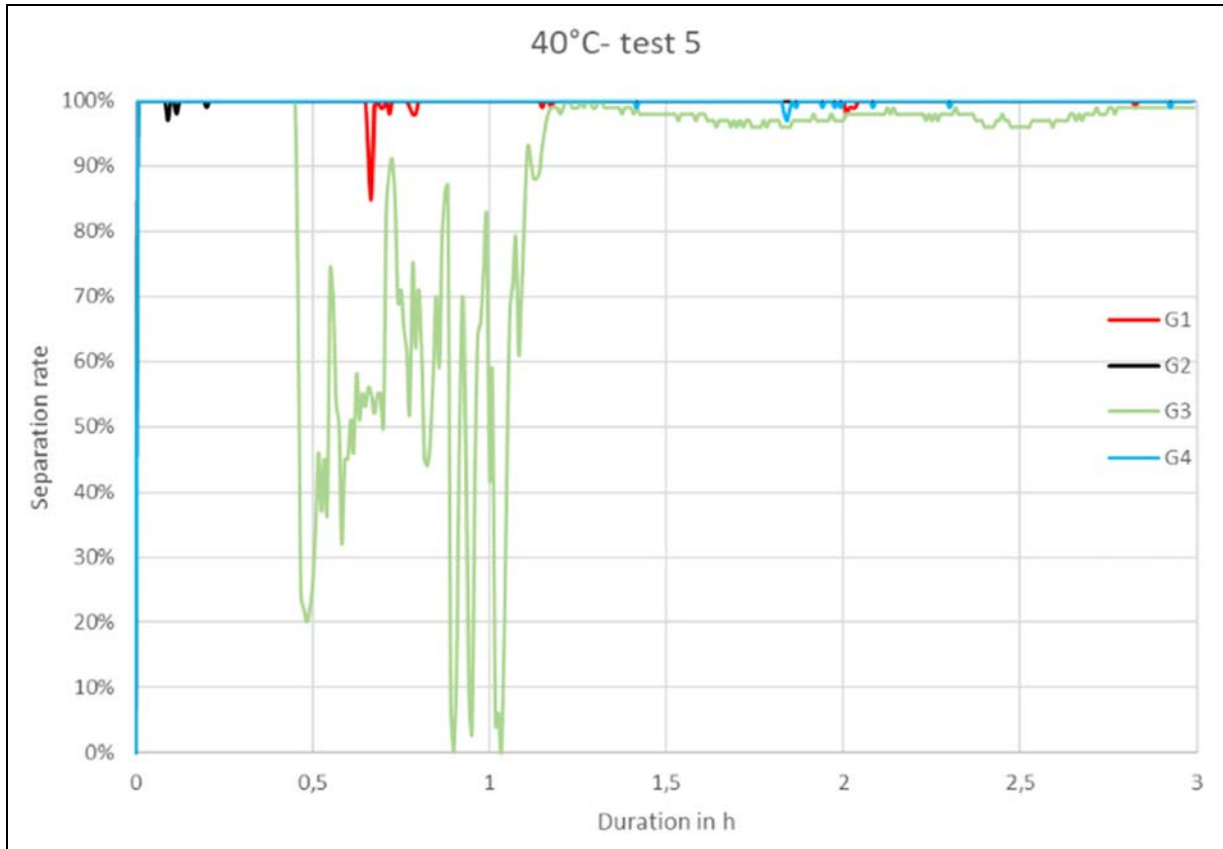


Figure 10. Film thickness for test number 5.

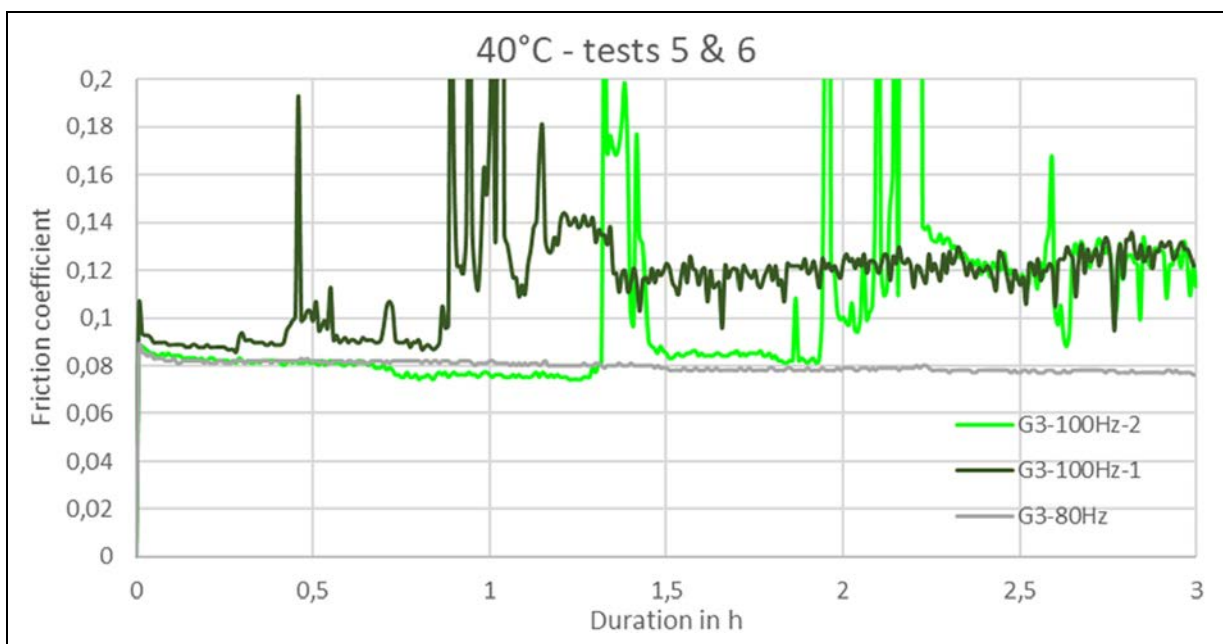


Figure 11. G3 friction coefficient for test numbers 5 and 6.

lead to starvation. The first step was to study greases at 40°C using condition number 5. Indeed, 40°C seems to be important to understand the grease behaviour. The friction coefficients are available in Figure 9.

Greases G1, G2 & G4 have exactly the same behaviour as in the previous conditions of Table 2 (Figure 4). Only a variation of friction coefficient between test conditions #1 and #5 is noticed due to speed. In addition, the surface separation is very satisfactory (Figure 10).

However, for grease G3 a major friction coefficient is obtained. Moreover, when this jump occurs, the separation goes to 0%, meaning, there is no lubricant between contacting parts. Starvation seems to occur in that case.

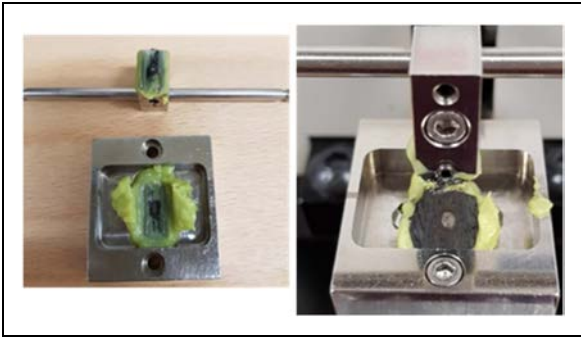


Figure 12. Wear G3 on HFRR.

In order to go further, another test at 80 Hz is carried out (test number 6) which reduces the speed and so the SD parameter (Table 4). Also this test is repeated at 100 Hz. (see Figure 11).

This phenomenon appears to be repeatable. A first jump appears, then the lubrication resumes and a second jump occurs. After these failures and due to surface degradation, the grease G3 is now the equivalent of a standard grease as G1. Indeed, it gives a friction coefficient equivalent or superior to G1 due to surface degradation. Also, it is frequency dependent. At 80 Hz, the phenomenon does not occur (Figure 11). Looking at it with the naked eye (figure 12), this major friction seems to involve a lot of particles inside the grease. The grease becomes black between the samples.

Now, at 80°C the same tests are performed (Figures 13 and 14).

There is no starvation compared to Figures 9 and 10. Indeed, here the friction coefficients are almost stable (Figure 13) and the film thickness is always above 50% (Figure 14). Finally, starvation occurs only at 40°C with grease G3.

To explain this wear (Figure 15) a test with condition 5 and G3 is repeated and stopped when the jump in friction coefficient occurs.

Wear scars were measured on the ball and disc after testing with grease G3 as shown in Figures 16 & 17.

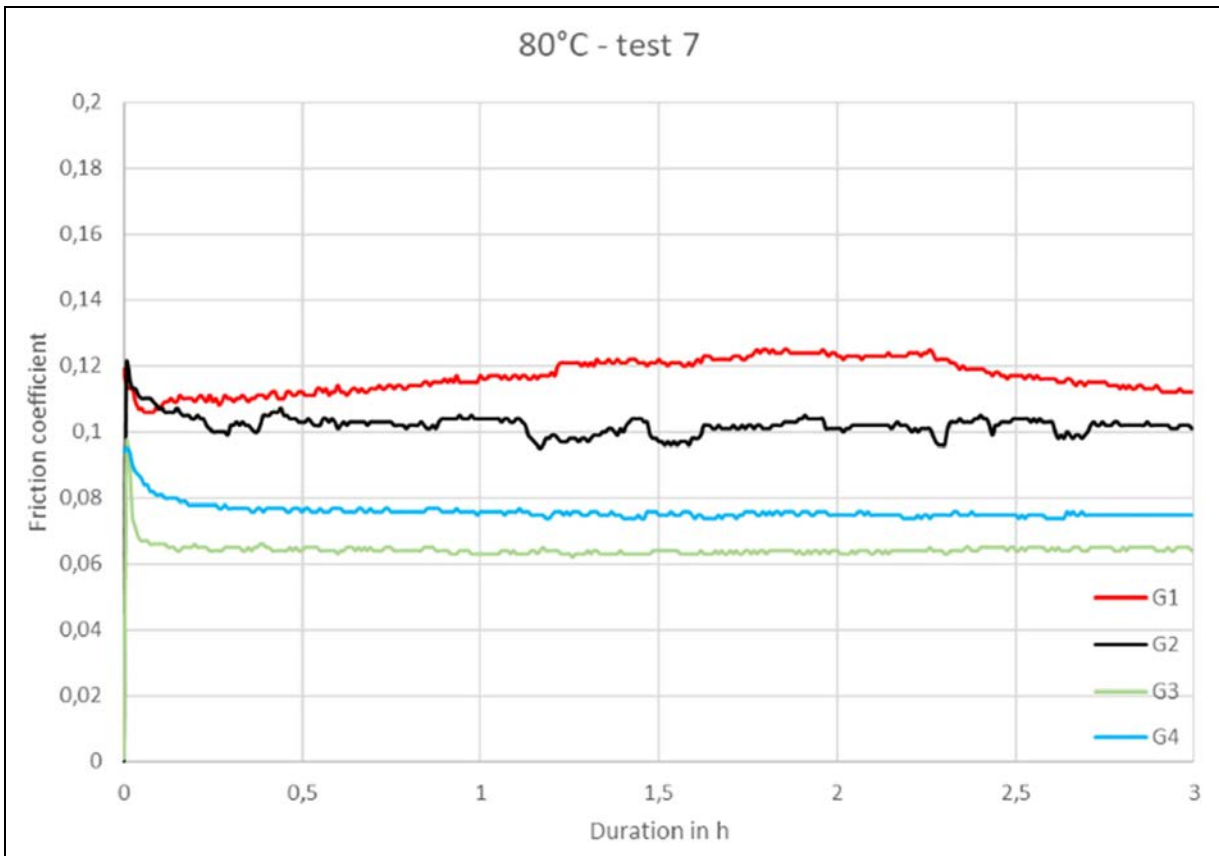


Figure 13. Friction coefficient for test number 7.

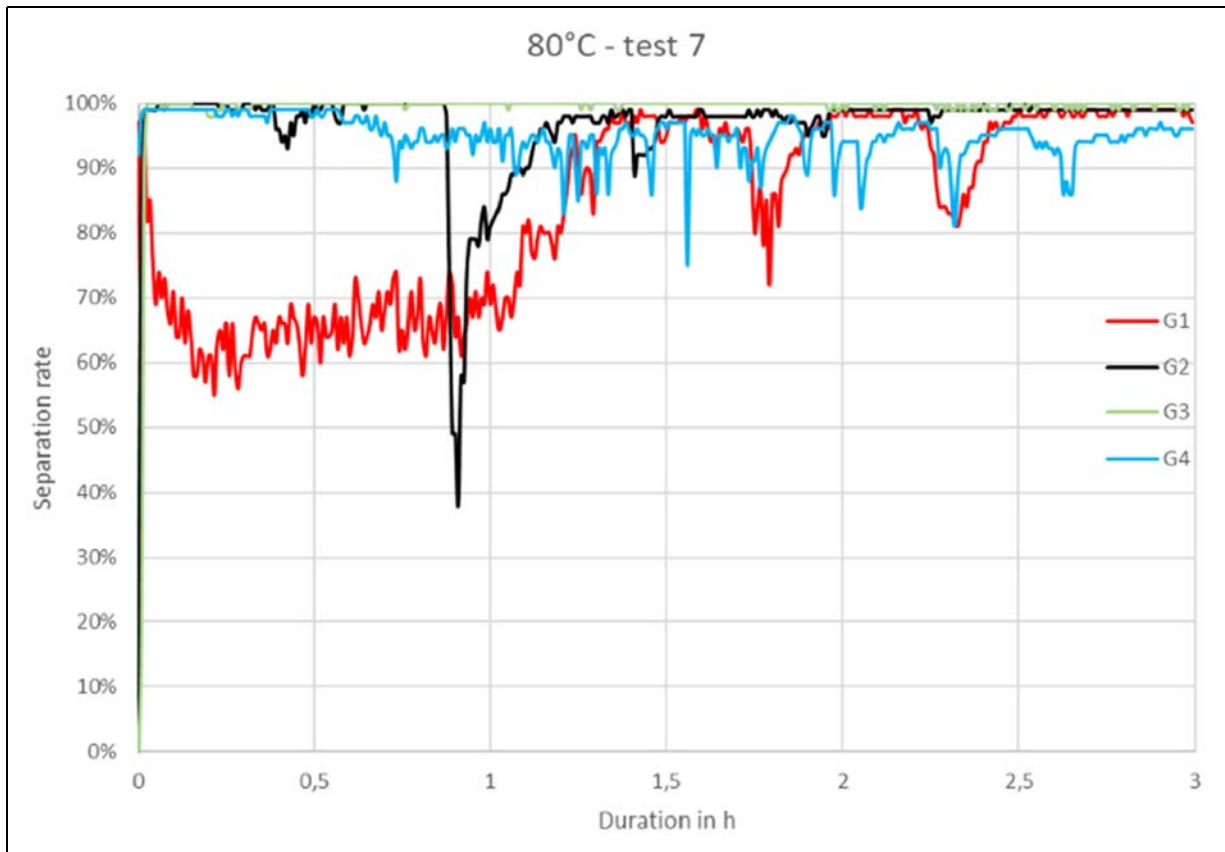


Figure 14. Film thickness for test number 7.

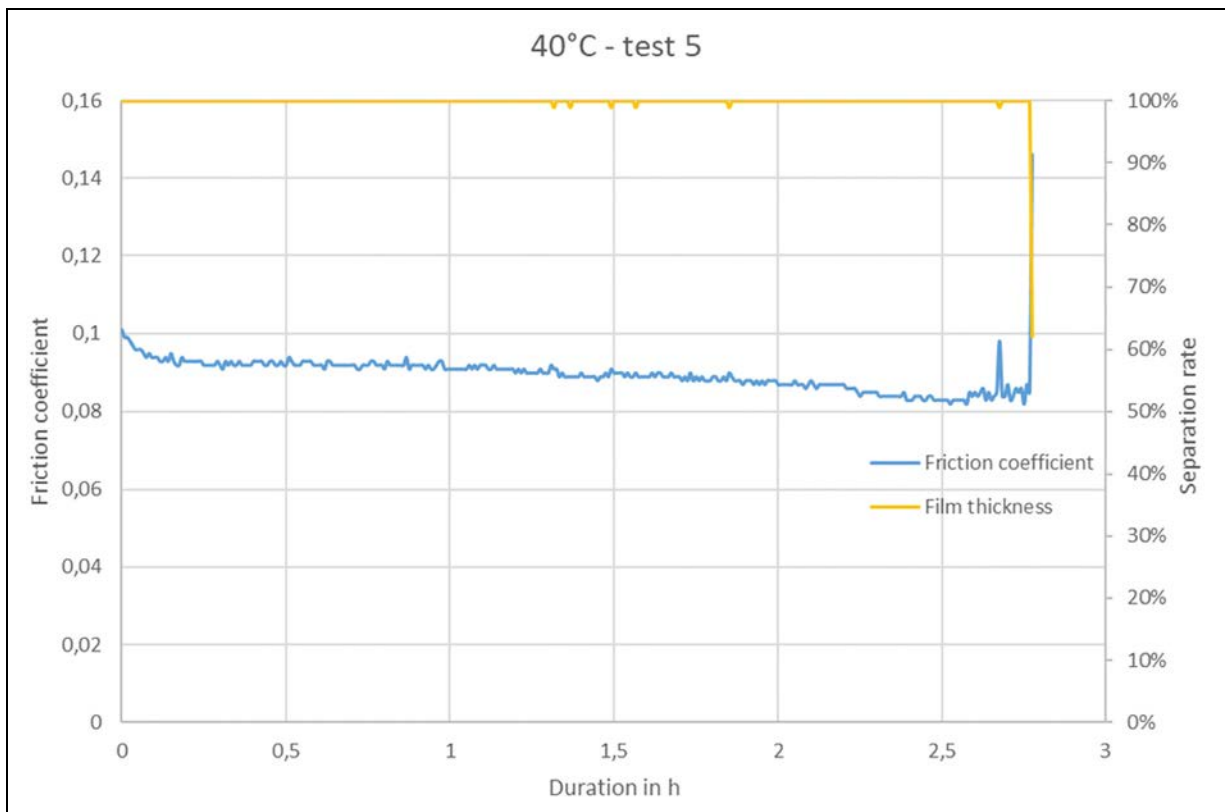


Figure 15. HFRR test stopped with G3 when jump occurs.

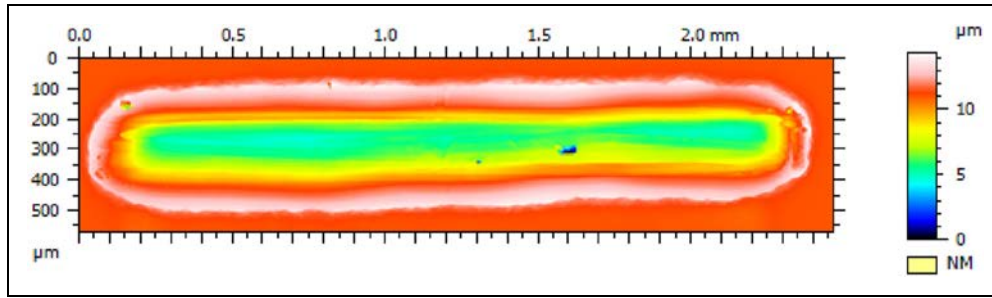


Figure 16. Disc scar.

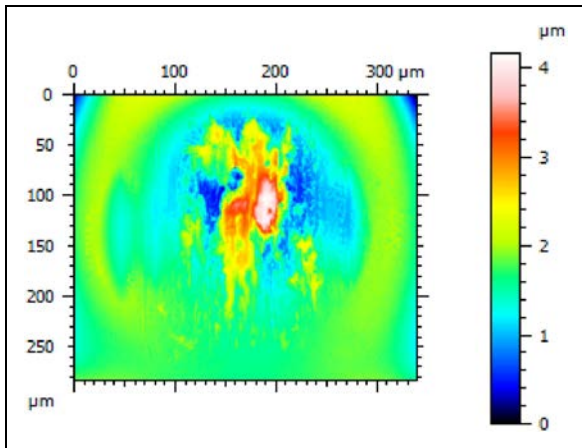


Figure 17. Ball scar.

It is possible to observe a material transfer from the disc (Figure 16) to the ball (Figure 17), which shows that, scuffing occurs with grease G3. The disc and ball weld and, with the movement imposed by the actuator, it transfers material onto the ball surface from the disc surface. Now, it could be interesting to study the influence of the grease composition directly on film thickness.

2.2. Film thickness study

On an EHL test rig, grease test repeatability is very difficult to obtain due to the chaotic behaviour of the grease¹⁵⁻¹⁷ even for exactly the same operating conditions and grease volumes. For conditions 7&8, the tests are repeated more than twice to obtain meaningful results. In this section, G1, G3 and G4 are studied as they have meaningful HFRR results.

In order to explain scuffing, the film thickness is measured as a function of time. The condition (8&9) seems relevant compared to previous tests (Table 2) due to velocity which seems to be the key parameter in this study. It can be compared to conditions 5&7 from table 3 of the HFRR section. The results for G1, G3 and G4 are available in Figures 18, 19 & 20 respectively.

First of all, it is interesting to note that for a same test a grease can have some chaotic but at the same time repeatable film thickness behaviour over time. For example, grease G1 at 40°C has 3 distinct behaviours (Figure 18). The first one separates correctly the surface around 250 nm. The second one is the opposite. The film thickness becomes smaller and approaches zero damaging the spaced layer coating of the test track on the disc and another one which oscillates between the 2 curves. This behaviour is very interesting. Indeed, it shows the ability of grease to replenish contact. The

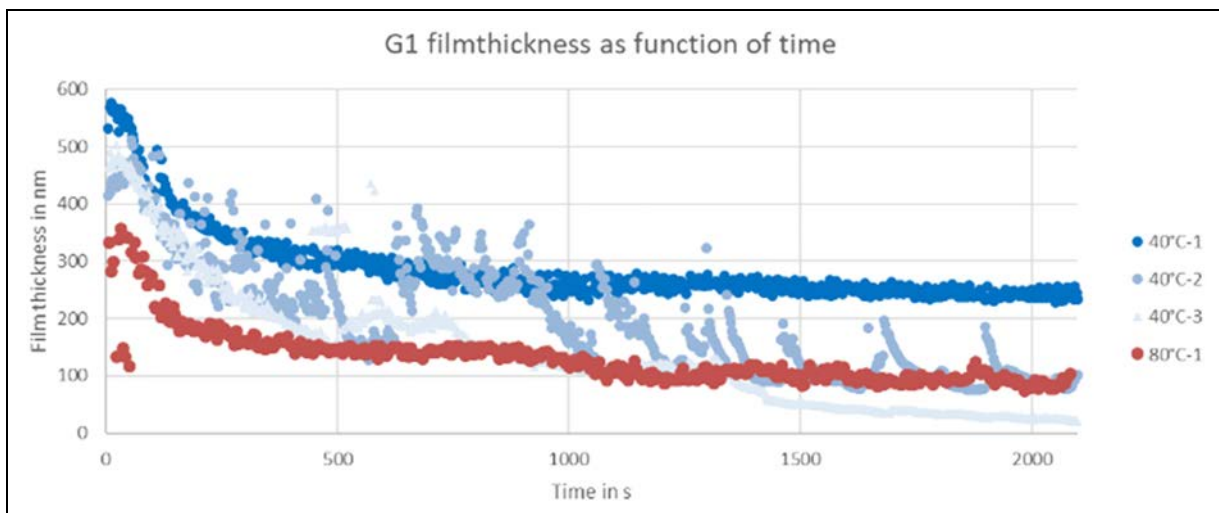


Figure 18. G1 results for conditions 8 & 9.

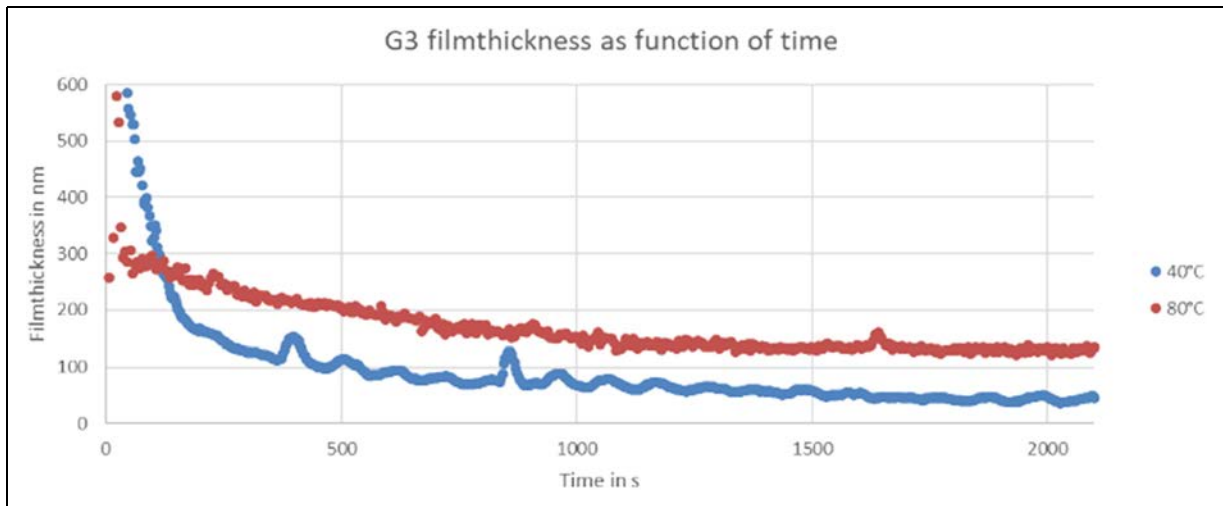


Figure 19. G3 results for conditions 8 & 9.

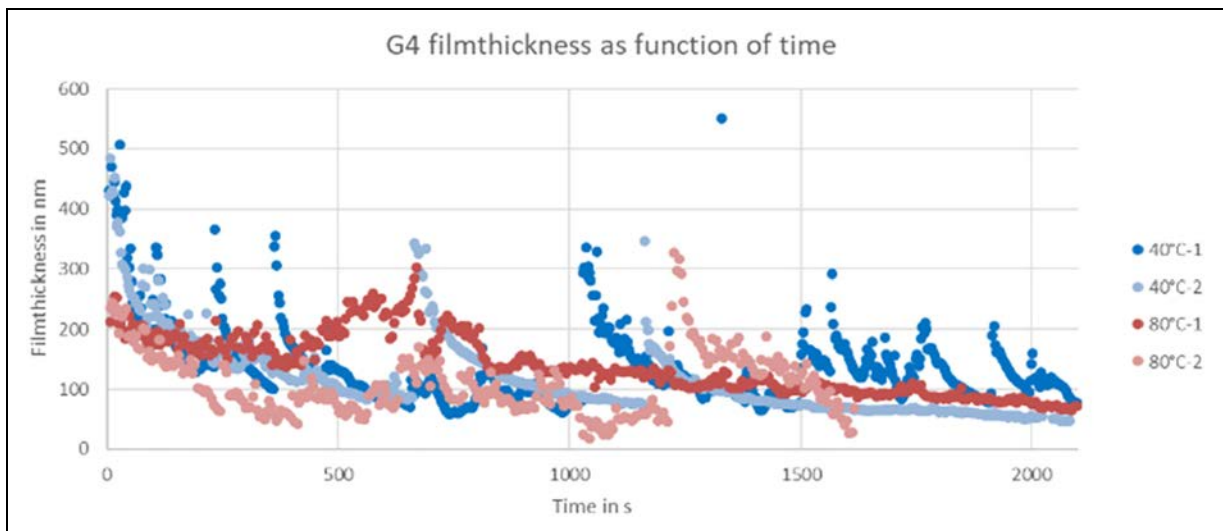


Figure 20. Figure 20. G4 results for conditions 8 & 9.

same ability is observable for G4 not only at 40°C but also at 80°C.

In order to investigate phenomenon from Figures 18 to 20, interferometric pictures of the contact area have been done. In Figure 21, images from EHD illustrate the contact state before and after replenishment. The rolling direction is indicated by a yellow arrow. When starvation begins in the left of top Figure 21, it could be observed starvation induced vibrations which promoted the replenishment (the sudden rise in film thickness of Figures 18–20).

However, this behaviour is not observed on G3. At 40°C, the film thickness decreases quickly and never recover unlike G4&G1. Finally, after some minutes, it goes to zero and damages the track. It is illustrated in Figure 22.

It is possible to observe the beginning of starvation on the right and left of the contact. However, the grease never replenishes contact and tends to a dry contact. It is similar to the behaviour found by other authors.¹⁸

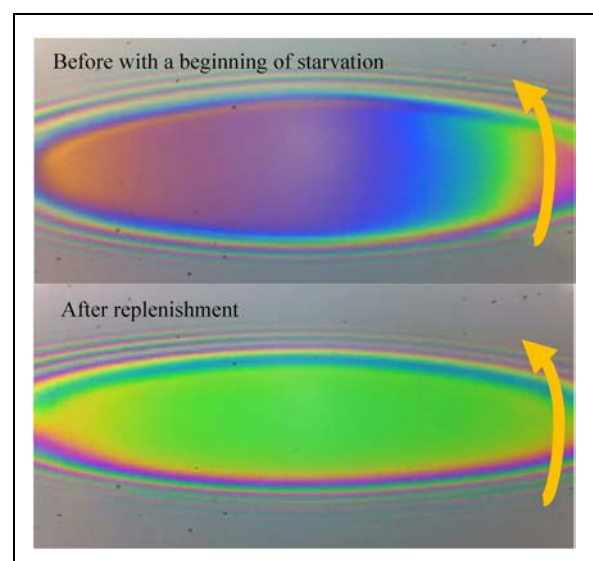


Figure 21. Contact replenishment with G4 at 40°C.

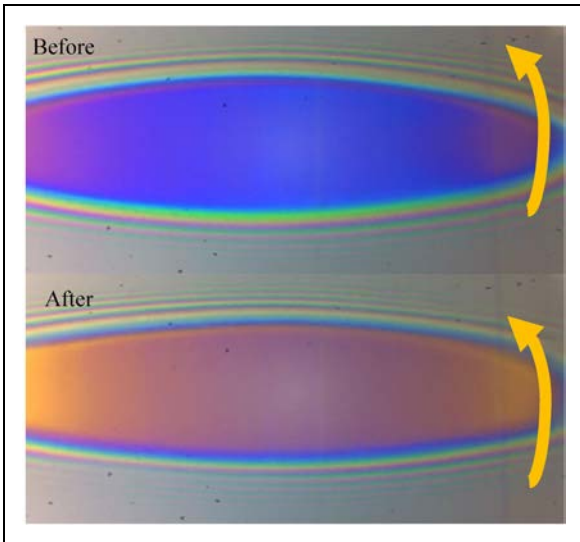


Figure 22. Contact starvation with G3 at 40°C.

On the contrary, at 80°C, the replenishment of this grease G3 greatly improves (temperature drops oil viscosity which improves the oil separation) and the film thickness at 80°C can even be higher than at 40°C, as shown in Figure 19.

2.3. Discussions

Grease G1, G2 & G4 were tested by 2 experimental devices. These devices which are complementary allow to study greases having friction coefficient, separation but also film thickness variation information.

It has been shown that G1 & G4 which have completely different composition in terms of additives concentration and couple oil + thickener have completely different friction behaviour. This composition variation which lead to double friction coefficient from G4 to G1, have no influence on scuffing.

Indeed, for G1 & G4, when the contact is at low values of film thickness, the grease can replenish the contact thanks to its properties even against centrifugal effects. For G1 at 80°C, the grease does not show the same ability. Nevertheless, the film thickness is lower than previous values due to the increase of temperature but it is more stable during the test, and the surface separation is improved protecting the surfaces too.

There are sporadic replenishments during tests. It is possible to explain:

- Starvation induces vibrations: these vibrations will allow the grease to move back inside the contact area
- Centrifugal effect: during tests, oil is stored on both sides of the contact. Due to centrifugal effect, the storage closer to the rotational shaft can supply the contact with the bleed oil.
- Mechanical degradation of the thickener matrix: degraded grease thickener insures a residual film on the rolling track.

All these phenomena improve re-flow until the next starvation event occurs.^{19,20}

On the contrary, although G3 & G4 have close composition, same SD, and performance except at 40°C with condition #5, it has been noticed that G3 at 40°C induces starvation in HFRR. This starvation leads to scuffing and so surface degradation. On EHD2 with G3 at 40°C, the film thickness events do not happen and therefore, the film generated shows a much smaller thickness, operating close to dry contact and hence, damaging the surface which can be the origin of scuffing found in section 2.1.3. However, it is interesting to note that G3 and G4 have the same oil (B) so the same viscosity. Also, in that case, the contact area and velocity are the same. To finish, the film thickness after 500 s at 40°C is almost the same. So, the parameters from starvation degree SD in oil-lubricated contacts is constant (table 4). This starvation criteria is not valid for grease as suggested by authors⁸. So, it could be interesting to consider oil separation measurements to study greased contact starvation as these are highly different for G3 & G4. Nevertheless, for these last greases the compositions and chemical and physical properties are similar, only the manufacturing process is different.

3. Conclusions

In The present study, it has been proved that grease composition and in particular additives can decrease friction. Adding MODTC and MOTDP in enough quantity can improve friction coefficient by 25% at 40°C. Also, changing the couple oil-thickener from a lithium-calcium complex with a mineral & PAO base oil to polyurea with Synthetic ester + PAO base oil allows friction to be decreased by 30% at 40°C.

However, if the contact frequency increases it is possible to observe starvation and so scuffing on surfaces using greases with the same oil, thickener technology and additives. It is important to note that the manufacturing process of polyurea thickener seems to play a key role on starvation on our case.

Borrowing the SD parameter from oil lubricated contact theory, it is possible to conclude that it is not sufficient to predict starvation on grease lubrication. Indeed, in this study, 2 greases with same oil viscosity, contact parameters leading to equivalent SD parameters give different behaviours due to very different oil separation. Indeed, when one grease insures correct lubrication, the other one induces starvation and so scuffing according to HFRR and EHD2 measurements.

In a future study, it could be interesting in order to predict starvation to modify the SD parameter with a physical notion of oil bleed using the IP121 method for example. To do this, it would be interesting to lead this future study by controlling more finely the parameters between the different greases. Also, it has been shown that temperature and contact frequency play a key role on starvation.

An application of this study can be rolling element lubrication from automotive drivetrains. A constant velocity joint uses grease in order to lubricate the contact between the roller and housing. Drivetrain greases are important

for automotive transverse drivetrains. It fills 2 main goals: lubricating the contact and extracting heat. In that case, the friction coefficient can be directly linked to the generated axial force of the tripod¹⁴. Friction between rollers and housing creates a force. The strength will depend on the friction coefficient and implies vibration on the car. These functions which are essential, insure the components have a long life²¹ avoiding starvation for example.

Acknowledgements

The authors would like to thank the ANRT (CIFRE N°2017/0094), STELLANTIS, the LaMCoS, in particular S. Wegeler, the Universidade do Porto (INEGI and FEUP) and the LTDS in particular C. Minfray and F. Dassenoy for their help and support.

Declaration of Conflicting Interests


The author(s) declared no potential conflicts of interest with respect to the research, authorship, and/or publication of this article.


Funding


The author(s) received no financial support for the research, authorship and/or publication of this article.

ORCID iDs

V Ripard  <https://orcid.org/0000-0003-2080-4893>

D Goncalves  <https://orcid.org/0000-0002-0549-3399>

Ville  <https://orcid.org/0000-0002-9743-8820>

J H O Seabra  <https://orcid.org/0000-0003-1919-0003>

References

- Lugt PM. A review on grease lubrication in rolling bearings. *Tribol Trans* 2009; 52: 470–480.
- Lugt PM, Velickov S and Tripp JH. On the chaotic behavior of grease lubrication in rolling bearings. *Tribol Trans* 2009; 52: 581–590.
- Muennich HC and Gloeckner HJR. Elastohydrodynamic lubrication of grease-lubricated rolling bearings. *A S L E Trans* 1980; 23: 45–52.
- GOHAR R and CAMERON A. Optical measurement of Oil film thickness under elasto-hydrodynamic lubrication. *Nature* 1963; 200: 458–459.
- Morales-Espejel GE, Lugt PM, Pasaribu HR, et al. Film thickness in grease lubricated slow rotating rolling bearings. *Tribol Int* 2014; 74: 7–19.
- Kaneta M, Ogata T, Takubo Y, et al. Effects of a thickener structure on grease elastohydrodynamic lubrication films. *Proc Inst Mech Eng Part J J Eng Tribol* 2000; 214: 327–336.
- Cann PME and Lubrecht AA. Bearing performance limits with grease lubrication: the interaction of bearing design, operating conditions and grease properties. *J Phys D Appl Phys* 2007; 40: 5446–5451.
- Cann PME, Damiens B and Lubrecht AA. The transition between fully flooded and starved regimes in EHL. *Tribol Int* 2004; 37: 859–864.
- Gonçalves DEP, Campos AV and Seabra JHO. An experimental study on starved grease lubricated contacts. *Lubricants* 2018; 6: 1–18.
- Nagata Y, Kalogiannis K and Glovnea R. Track replenishment by lateral vibrations in grease-lubricated EHD contacts. *Tribol Trans* 2012; 55: 91–98.
- Dr Gareth Fish. The Effect of Friction Modifier additives on CVJ Grease Performance. NLGI Spokesm. 2002;66:22-31. Accessed July 19, 2018. <https://www.nlgi.org/downloads/the-effect-of-friction-modifier-additives-on-cvj-grease-performance/>.
- AFNOR. Produits pétroliers et graisses lubrifiantes - Séparation d'huile au stockage des graisses lubrifiantes - Méthode sous pression - Conditions statiques. NF T60-191. Published online 2011:12. Accessed December 3, 2018. <https://viewer.afnor.org/Pdf/Viewer/?token=UoEbseQe0bo1>.
- Ripard V. Tribological characterization of greased drive-shaft: Evaluation of constant velocity joint durability. Published online 2019. <http://www.theses.fr/2019LYSEI083/document>.
- Serveto S, Mariot J-P and Diaby P. Joint tripode couissant de transmission automobile. Effort axial généré : essais et modèles. In: *18eme Congrès Français de Mécanique*. ; 2007:6. Accessed May 9, 2017. <http://documents.irevues.inistfr/bitstream/handle/2042/15759/CFM2007-0296.pdf?sequence=1>.
- Cen H and Lugt PM. Film thickness in a grease lubricated ball bearing. *Tribol Int* 2019; 134: 26–35.
- Lugt PM, Velickov S and Tripp JH. Tribology transactions On the chaotic behavior of grease lubrication in rolling bearings On the chaotic behavior of grease lubrication in rolling bearings. *Tribol Trans* 2009; 52: 581–590.
- Svoboda P, Kostal D, Kunak J, et al. Study of grease behaviour in a starved elastohydrodynamically lubricated contact. *MM Sci. J* 2014; 2: 465–469.
- Huang L, Guo D and Shizhu W. Film thickness decay and replenishment in point contact lubricated with different greases: a study into oil bleeding and the evolution of lubricant reservoir. *Tribol Int* 2016; 93: 620–627.
- Cann PM. Starvation and reflow in a grease-lubricated elastohydrodynamic contact. *Tribol Trans* 1996; 39: 698–704.
- Cann PME. Thin-film grease lubrication. *Proc Inst Mech Eng Part J J Eng Tribol* 1999; 213: 405–416.
- Lee C-H, Choi JY, Jeon IS, et al. Grease degradation in constant velocity (CV) joints. *Tribol Trans* 2011; 54: 825–831. doi:10.1080/10402004.2011.606958
- ASTM International. Standard Test Methods for Cone Penetration of Lubricating Grease. Published online 2017. Accessed June 5, 2019. <https://www.astm.org/Standards/D217.htm>.